

WAKEFIELD CALCULATIONS FOR SEPTUM MAGNET IN LCLS-II*

K.L.F. Bane, T. Raubenheimer, SLAC, Menlo Park, CA 94025, USA

INTRODUCTION

The LCLS-II would have delivered low emittance beams with an energy in the range 7–13.5 GeV to one of two undulators, one for generating soft x-rays (SXR) and the other for hard x-rays (HXR) [1]. To allow for flexibility in the distribution of the beams to the two undulators, a fast kicker and Lambertson-type septum magnet would be installed just upstream of the undulator region. The septum itself is 2 m long and the beam is meant to traverse it while passing within millimeters of metallic walls, which will induce resistive wall wakefields. The longitudinal wakes will take energy from the beam and add a longitudinally correlated energy variation—an energy chirp. The transverse wakefields can increase the beam’s projected emittance.

In this report we perform calculations of the longitudinal and transverse wakefields of the septum, find their effects on the beam, and put the results in the context of the wakes of other objects in the downstream part of LCLS-II.

Figure 1 gives the layout of the LCLS-II beamlines upstream of the undulators, showing the location of the fast kicker and septum magnets. The septum magnet geometry we consider is shown in Fig. 2. The design orbit for the un-kicked (free) beam is 1.6 mm above a curved SS surface; the (horizontally) kicked beam moves in the middle of a flat, rectangular chamber with a vertical aperture of 5 mm.

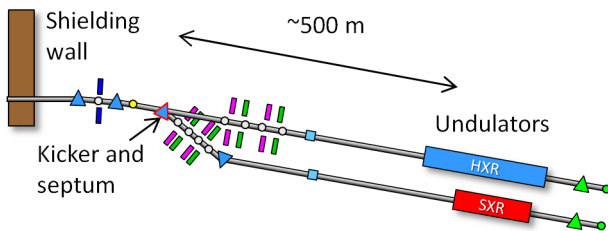


Figure 1: Layout of the LCLS-II beamlines in the vicinity and downstream of the fast kicker and septum magnet [2].

WAKES OF SHORT BUNCHES

Four bunch scenarios are considered for the operation of LCLS-II: short, relatively flat distributions with bunch charge $eN = 250, 60, 12, 50$ pC; peak current $\hat{I} = 3, 3, 3, 4$ kA; full width $t_{fw} = 70, 15, 3, 10$ fs. With the peak current (relatively) fixed and the bunches quite short, the wake strength of a bunch tends to vary $\sim t_{fw}$ —since the wake is normalized to total charge eN . Thus it is the first scenario, the so-called “high charge” case with $eN = 250$ pC that will induce the largest wake effects by far, and

* Work supported by the U.S. Department of Energy under contract DE-AC02-76SF00515.

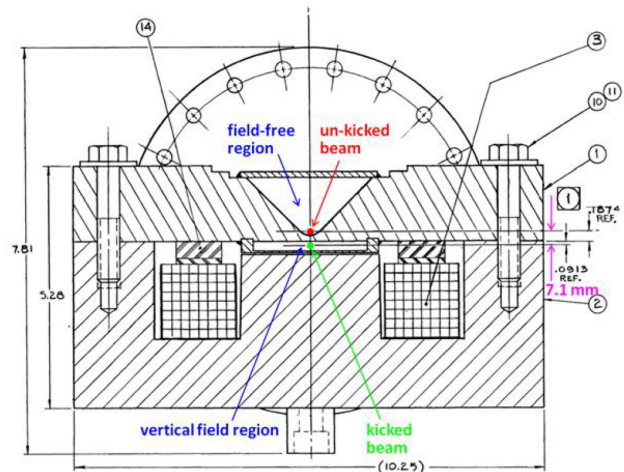


Figure 2: Cross-section the horizontally deflecting Lambertson septum magnet, “HLAM”, considered in this report. The length of the chamber is 2.2 m. (Dimensions in the figure, unless otherwise specified, are in inches.)

in this report we limit our study to this case. The bunch distribution $I(s)$, to be used in calculations, is taken from the LCLS and is shown in Fig. 3 (the blue curve); note that the head is to the left, at positions $s < 0$. The distribution is double-horned, with an rms length $\sigma_z = 6.1 \mu\text{m}$; its core can be approximated by a uniform 3 kA (the red curve). Presumably, for the FEL we would like the entire beam core to reach saturation in the undulator together; thus the wake effects over the bunch core are most important.

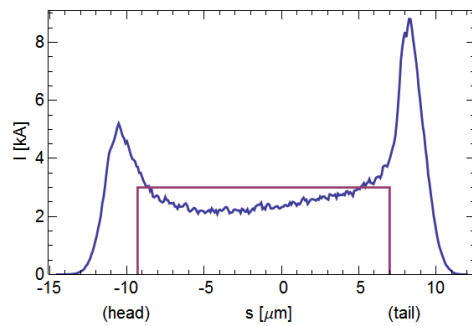


Figure 3: The bunch distribution used in the simulations, which represents the “high charge,” 250 pC case (blue), and a uniform approximation of the core at 3 kA (red).

The energy variation induced in a bunch by the wake is

$$E_w(s) = -\frac{L}{c} \int_0^\infty W_z(s') I(s - s') ds', \quad (1)$$

with L the structure length, c the speed of light, and $W_z(s)$ the longitudinal point charge wake ($W_z > 0$ means energy loss). The point charge wake of a periodic structure has a maximum value at $s = 0^+$. In a round structure that value is $W_z(0^+) = Z_0 c / (\pi a^2)$, with $Z_0 = 377 \Omega$ and a the minimum radius of the boundary [3]. Similarly, for the dipole wake, for which $W_y(0) = 0$, the slope at origin is limited to $W'_y(0^+) = 2Z_0 c / (\pi a^4)$. For non-round structures the scaling will be the same but the constant factor will differ.

For bunches that are short compared to the zero-crossing distance of the wake, Eq. 1 can be approximated by $E_w(s) \approx -LW_z(0^+)Q(s)$, with $Q(s) = \int_{-\infty}^s I(s') ds' / c$. If, in addition, the core of the distribution is uniform, then over the core, $Q(s) \sim s$ and the wake-induced energy chirp will be approximately linear, with negative slope.

SEPTUM MAGNET

Free Beam

The resistive wall wakefields are weak forces for long bunches, *i.e.* when $\sigma_z \gg s_0 \equiv (2a^2/Z_0\sigma_c)^{1/3}$, where a is the offset of the beam from the wall, and σ_c is the conductivity of the wall metal. For the free, HXR beam, we find that $\sigma_z \ll s_0 = 21 \mu\text{m}$ ($a = 1.6 \text{ mm}$, $\sigma_c = 1.4 \times 10^6 \Omega^{-1}\text{m}^{-1}$ for SS), and the effect is strong. In a round chamber, the longitudinal point charge wake (in the dc approximation) is given by [4]

$$W_z(\zeta) = \frac{4Z_0c}{\pi a^2} \left(\frac{e^{-\zeta}}{3} \cos \sqrt{3}\zeta - \frac{\sqrt{2}}{\pi} \int_0^\infty \frac{x^2 e^{-x^2\zeta}}{x^6 + 8} dx \right) \quad (2)$$

with $\zeta = s/s_0$.

However, the chamber surrounding the free beam is only partially round, at the bottom (see Fig. 2). K. Yokoya has found the solution of the resistive wall wake for any boundary shape [5]. The solution is given in terms of an integral equation that he then solves numerically in a computer program. We use his program to find the wakes excited by the beam. In Fig. 4 we show in cross-section the lower part of the actual chamber shape (in red), the modified chamber that we use as boundary in our calculation (in blue), and the nominal position of the free beam (the olive dot).

The calculation results are given in Fig. 5. In frame (a) we present the point charge wake $W_z(s)$ for the model structure (blue), and the wake if the entire boundary were a circle of radius $a = 1.6 \text{ mm}$ (blue dashed, Eq. 2). Because of the vertical asymmetry in geometry, the energy loss varies linearly with vertical offset. However, for reasonable offsets ($\Delta y < 100 \mu\text{m}$) Yokoya's program finds that the change in wake is small.

Using Eq. 1 we obtain the energy variation in the bunch, $-E_w(s)$ [Figure 5(b)]. We see that the energy varies rather linearly over the bunch core, with a total $\Delta E_w = 1.3 \text{ MeV}$; over the entire bunch the variation is $\Delta E_w = 2.6 \text{ MeV}$. In the two frames we show also the wake and its effect if the surface were plated with Cu (the red curves). This reduces ΔE_w to 0.4 (0.7) MeV over the core (the entire beam).

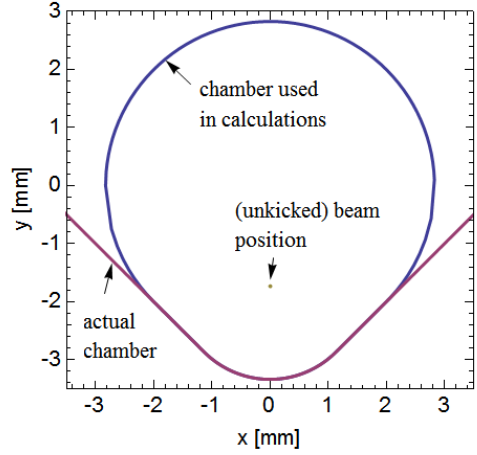


Figure 4: Position of unkicked beam, its relation to the chamber wall, and the model chamber used in calculations.

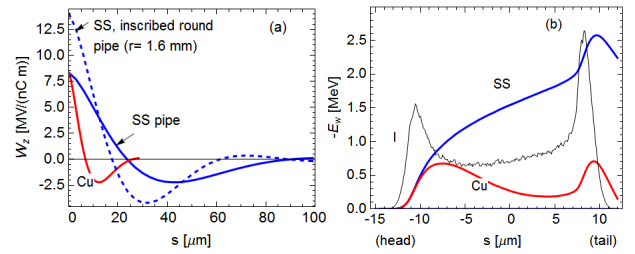


Figure 5: For the free beam: (a) Point charge wake in the SS structure (blue), if it were Cu plated (red); for an inscribed round pipe with SS, shown for comparison (dashes). (b) Total wake energy change for $eN = 250 \text{ pC}$ case. Bunch shape I is also shown (gray).

Transverse Wake

For our structure, with mirror symmetry in x and no symmetry in y , the transverse wake between two particles can be written as

$$\begin{aligned} W_y(s, y_1, y_2) &= W_{y0}(s) + y_1 W_{yd}(s) + y_2 W_{yq}(s) \\ W_x(s, x_1, x_2) &= x_1 W_{xd}(s) - x_2 W_{yq}(s) \end{aligned} \quad (3)$$

where x, y , indicate (small) offsets from the design orbit, and subscript 1 (2) refers to the leading (trailing) particle. Even on the design orbit, the vertical wake induced by the beam, $W_{y0}(s)$, will kick the beam downward and increase its projected emittance. The other wake functions $W_{xd}(s)$, $W_{yd}(s)$, $W_{yq}(s)$, are dipole and quad wake components. Yokoya's program finds all these components.

In Fig. 6(a) we plot the numerically obtained $-W_{y0}(s)$ (the blue curve). Convolving again like in Eq. 1 and dividing by the energy E , we obtain the kick angle $\Delta y'$. With normalized emittance $\epsilon_n = 0.4 \mu\text{m}$, $E = 7 \text{ GeV}$, $\beta_y = 30 \text{ m}$, then $\sigma_{y'} = 1 \mu\text{r}$. The normalized kick $\Delta y' / \sigma_{y'}$ is plotted in Fig. 6(b) (the blue curve); the average and rms values are 0.74, 0.54. The projected emittance growth on

the design orbit is comparable to the slice emittance! Plating the septum wall with Cu can greatly reduce the effect (the red curves in Fig. 6). The relative average and rms kick values become 0.21, 0.11.

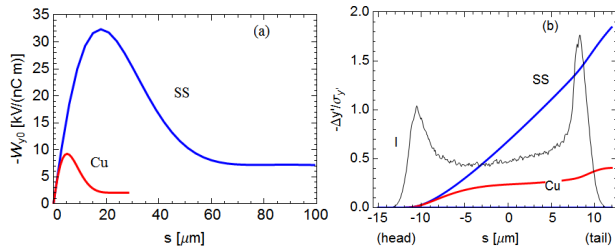


Figure 6: For the free beam: (a) Point charge vertical wake (on the design orbit) in the SS structure (blue) and if it were Cu plated (red). (b) Relative total vertical kick angle for $eN = 250$ pC case. Bunch shape I is also shown (gray).

The dipole wake functions W_{xd} , W_{yd} , were also computed. In an FEL the allowable pulse-to-pulse variation in orbit is similar to the beam size, which in the septum region is $\sigma_y = 30 \mu\text{m}$. Repeating the previous exercise with W_{yd} for a beam offset by σ_y , we find that the average and rms values of $\Delta y'/\sigma_y$ are 0.01, 0.01, for SS, which are negligible (the results for W_{xd} are similar). As to the quad wake W_{yq} , it defocuses in y and is weak: the minimum effective focal length (near the tail of the bunch) is 6.5 km.

Kicked Beam

The SXR beam passes near the center of a rectangular chamber of width 76 mm and height 5 mm; its trajectory is bent horizontally. The bottom and sides are SS, the top is low carbon steel ($\sigma_c = 10^7 \Omega^{-1}\text{m}^{-1}$). For simplicity we will take as model parallel SS plates. The results will be slightly pessimistic for the longitudinal effect, and will miss the vertical kick on the symmetry plane (which we expect to be small).

The point charge wakefields between parallel, resistive plates have long been known [6, 7]. However, for convenience, we use Yokoya's program here again. In the flat case, the longitudinal wake at the origin, for plates separated by $2a$, is smaller than for the round case (with radius a) by the factor $\pi^2/16$. Performing the same calculations as for the free beam we find that the induced energy change E_w is similar to that given in Fig. 5(b) (the blue curve), though the amplitude is here about half as large. The energy variation over the bunch core (entire bunch) $\Delta E_w = 0.7$ (1.3) MeV.

The transverse wake for the parallel plate model follows Eq. 3, with $W_{y0} = 0$, $W_{xd}(s) = W_{yq}(s)$. In flat geometry $W_{yd}(s) \approx W_{yq}(s)$ over short distances. For a beam offset by σ_y , the maximum wake kick $\Delta y'/\sigma_y$ (at the back of the bunch) is 0.02, with an average of 0.01, again a small effect. The quad wake defocuses vertically and is weak: the minimum focal length (at the back of the bunch) is 1 km.

The dispersion for the kicked beam can turn the wake

induced energy spread into emittance growth as: $\delta\epsilon_x \approx \beta_x \eta_x'^2 \sigma_{\delta w}^2 / (2\epsilon_x)$, with η_x' the derivative of the dispersion function and $\sigma_{\delta w}$ the relative rms energy spread due to the wake. Taking $\beta_x = 36$ m, $\eta_x' = 7 \times 10^{-3}$, $\sigma_{\delta w} = 0.7 \text{ MeV} / (2\sqrt{3}E) = 3 \times 10^{-5}$, we obtain $\delta\epsilon_x = 0.03$, a negligible growth.

DISCUSSION

In Table 1 we show how the wake-induced energy variation ΔE_w in the septum compares with that in other vacuum chamber regions of LCLS-II downstream of the last bunch compressor, BC2: in the 580 m of Linac 3, the bypass line (1200 m), the linac-to-undulator transfer line (LTU) (300 m), and the undulator blank (in the HXR beam line) (170 m). Considering the septum is only 2.2 m long, its wake effect is relatively strong (assuming SS)—due to the extremely small chamber aperture. Note that for the septum as well as for the other regions in the table, the chirp is negative and mostly linear. In the LCLS-II the total wake-induced chirp serves an important function—to compensate the energy chirp left in the beam in BC2.

Finally, an important conclusion of this work is that, in order to avoid wake induced emittance growth, the septum surface in the vicinity of the free-beam orbit should be plated with a good conductor like Cu, even if the longitudinal wake adds a small nonlinearity to the energy chirp.

Table 1: Wake-induced Energy Variation ΔE_w in Different Regions of LCLS-II after BC2, for the High charge Case, $eN = 250$ pC [8]. Results are Given for the Core of the Beam, and the Entire Beam. The Septum Results Assume SS.

Region	Core	Total
Linac 3	19.8 MeV	36.0 MeV
Bypass	7.1	12.5
LTU	5.9	10.0
Septum, Free Beam	1.3	2.6
Undulator Blank	2.6	7.8
Total	36.7 MeV	68.9 MeV

ACKNOWLEDGEMENT

We thank K. Yokoya for supplying us with his Fortran program for calculating resistive wall wakes, and Y. Ding for providing the bunch shape used in the calculations.

REFERENCES

- [1] LCLS-II Conceptual Design Report, SLAC-R-978, 2011.
- [2] LCLS-II CD2 Lehman DOE Review, 21 August 2012, SLAC.
- [3] See e.g. discussion in K. Bane and G. Stupakov, Phys. Rev. ST-AB 6 (2003) 024401.
- [4] A. Chao, *Physics of collective beam instabilities in high energy accelerators*, (John Wiley & Sons, 1993) 47.
- [5] K. Yokoya, Part. Accel. 41 (1993) 221, and KEK-PREPRINT-92-196.
- [6] H. Henke and O. Napoly, Proc. EPAC90, p. 1046, 1990.
- [7] K. Bane and G. Stupakov, Proc. PAC05, p. 3390, 2005.
- [8] K. Bane, "Short-range, longitudinal wakefield effects in LCLS-II," talk at LCLS-II meeting, SLAC, June 2012.